haematologica
Journal of The Ferrata Storti Foundation

Genetic and phenotypic characterization of indolent T-cell lymphoproliferative disorders of the gastrointestinal tract

by Craig R. Soderquist, Nupam Patel, Vundavalli V. Murty, Shane Betman, Nidhi Aggarwal, Ken H. Young, Luc Xerri, Rebecca Leeman-Neill, Suzanne K. Lewis, Peter H. Green, Susan Hsiao, Mahesh M. Mansukhani, Eric D. Hsi, Laurence de Leval, Bachir Alobeid, and Govind Bhagat

Haematologica 2019 [Epub ahead of print]

Citation: Craig R. Soderquist, Nupam Patel, Vundavalli V. Murty, Shane Betman, Nidhi Aggarwal, Ken H. Young, Luc Xerri, Rebecca Leeman-Neill, Suzanne K. Lewis, Peter H. Green, Susan Hsiao, Mahesh M. Mansukhani, Eric D. Hsi, Laurence de Leval, Bachir Alobeid, and Govind Bhagat. Genetic and phenotypic characterization of indolent T-cell lymphoproliferative disorders of the gastrointestinal tract.
Haematologica. 2019; 104:xxx
doi:10.3324/haematol.2019.230961

TITLE PAGE

Concise Title: Genetic and phenotypic characterization of indolent T-cell lymphoproliferative disorders of the gastrointestinal tract

Short Running Title: Genetic alterations in indolent GI T-cell LPDs

Authors: Craig R. Soderquist[1], Nupam Patel[1], Vundavalli V. Murty[1], Shane Betman[1], Nidhi Aggarwal[2], Ken H. Young[3], Luc Xerri[4], Rebecca Leeman-Neill[1], Suzanne K. Lewis[5], Peter H. Green[5], Susan Hsiao[1], Mahesh M. Mansukhani[1], Eric D. Hsi[6], Laurence de Leval[7], Bachir Alobeid[1], and Govind Bhagat[1].

Institutional Affiliation:

[1]Department of Pathology and Cell Biology, Columbia University Irving Medical Center, New York Presbyterian Hospital, New York, NY, United States; [2]Department of Pathology, University of Pittsburgh Medical Center, Pittsburgh, PA, United States, [3]Department of Hematopathology, MD Anderson Cancer Center, Houston, TX, United States, [4]Department of Bio-Pathology, Institut Paoli-Calmettes, Aix-Marseille University, Marseille, France, [5]Department of Medicine, Celiac Disease Center, Columbia University Irving Medical Center, New York Presbyterian Hospital, [6]Pathology and Laboratory Medicine Institute, Cleveland Clinic, Cleveland, OH, United States; [7]Institute of Pathology, Lausanne University Hospital (CHUV), Lausanne, Switzerland.

Corresponding authors:

Author: Craig Soderquist MD

Address: Department of Pathology and Cell Biology, Columbia University Irving Medical Center, New York Presbyterian Hospital

VC14-240E

630 West 168th Street

New York, NY 10032

email: crs2130@cumc.columbia.edu

Author: Govind Bhagat MD

Address: Department of Pathology and Cell Biology, Columbia University Irving Medical Center, New York Presbyterian Hospital

VC14-228
630 West 168th Street
New York, NY 10032
email: gb96@cumc.columbia.edu

Abstract

Indolent T-cell lymphoproliferative disorders of the gastrointestinal tract are rare clonal T-cell diseases that more commonly occur in the intestines and have a protracted clinical course. Different immunophenotypic subsets have been described, but the molecular pathogenesis and cell of origin of these lymphocytic proliferations is poorly understood. Hence, we performed targeted next-generation sequencing and comprehensive immunophenotypic analysis of 10 indolent T-cell lymphoproliferative disorders of the gastrointestinal tract, which comprised CD4+ (n=4), CD8+ (n=4), CD4+/CD8+ (n=1) and CD4-/CD8- (n=1) cases. Genetic alterations, including recurrent mutations and novel rearrangements, were identified in 8/10 (80%) lymphoproliferative disorders. The CD4+, CD4+/CD8+, and CD4-/CD8- cases harbored frequent alterations of the JAK-STAT pathway genes (5/6, 82%); *STAT3* mutations (n=3), *SOCS1* deletion (n=1) and *STAT3-JAK2* rearrangement (n=1), and 4/6 (67%) had concomitant mutations in epigenetic modifier genes (*TET2*, *DNMT3A*, *KMT2D*). Conversely, 2/4 (50%) of the CD8+ cases exhibited structural alterations involving the 3' untranslated region of the *IL2* gene. Longitudinal genetic analysis revealed stable mutational profiles in 4/5 (80%) cases and acquisition of mutations in one case were a harbinger of disease transformation. The CD4+ and CD4+/CD8+ lymphoproliferative disorders displayed heterogeneous Th1 (T-bet+), Th2 (GATA3+) or hybrid Th1/Th2 (T-bet+/GATA3+) profiles, while the majority of CD8+ disorders and the CD4-/CD8- disease showed a type-2 polarized (GATA3+) effector T-cell (Tc2) phenotype. Additionally, CD103 expression was noted in 2/4 CD8+ cases. Our findings provide insights into the pathogenetic bases of indolent T-cell lymphoproliferative disorders of the

gastrointestinal tract and confirm the heterogeneous nature of these diseases. Detection of shared and distinct genetic alterations of the JAK-STAT pathway in certain immunophenotypic subsets warrants further mechanistic studies to determine whether therapeutic targeting of this signaling cascade is efficacious for a proportion of patients with these recalcitrant diseases.

Introduction

Non-Hodgkin lymphomas frequently occur in the gastrointestinal (GI) tract, with the majority representing B-cell neoplasms[1–3]. T-cell lymphomas account for 10-20% of all primary GI lymphomas[1–3]. Aggressive lymphomas, including enteropathy-associated T-cell lymphoma (EATL) and monomorphic epitheliotropic intestinal T-cell lymphoma (MEITL), are among the more common types of primary GI T-cell lymphomas, which are associated with high morbidity and mortality[1,4,5]. In recent years, there has been a growing awareness of indolent T- and NK-cell lymphoproliferative disorders that can also arise within the GI tract and involve a variety of GI organs[6,7]. The pathogenesis of indolent NK-cell disorders is unclear and it is not yet known if they constitute neoplastic proliferations of NK-cells[7]. Indolent T-cell lymphoproliferative disorders (ITLPDs) of the GI tract, which constitute an immunophenotypically diverse group of clonal T-cell diseases, have been better characterized and hence included as provisional entities in the revised 4th edition of the World Health Organization (WHO) classification of lymphoid neoplasms[1]. The clinical, morphological, and immunophenotypic features of ITLPDs of the GI tract differ from other types of primary GI T-cell lymphomas[6,8–16] and their cellular derivation, although not well established, is also considered to be distinct[9,11]. Overlapping genomic and genetic alterations have been reported in EATL and MEITL[17–21]. Limited data suggest a different spectrum of genomic aberrations in ITLPDs of the GI tract[11,13], and until recently, no recurrent genetic abnormality had been identified in these disorders[15]. However, the mutational landscape and molecular pathways underlying the initiation and progression of ITLPDs of the GI tract are unknown and the cell of origin of the different immunophenotypic subsets has not been

defined. To gain further insights into the biology of these rare diseases, we performed comprehensive immunohistochemical, molecular and targeted next-generation sequencing analyses of a series of 10 cases.

Methods

Case selection

The pathology department databases of multiple institutions were searched for primary gastrointestinal T-cell lymphomas, over a 23 year period (1996-2018), to identify cases fulfilling histopathologic and clinical criteria of ITLPDs as defined in the revised WHO classification[1]. Clinical data, including therapy and outcomes, were obtained from the treating physicians or electronic medical records. The study was performed in accordance with the principles of the Declaration of Helsinki and protocols approved by the Institutional Review Boards of the participating institutions.

Morphology and immunophenotypic analysis

Hematoxylin and Eosin (H&E) stained formalin-fixed, paraffin-embedded (FFPE) biopsy sections were reviewed to assess cyto-architectural features. Immunohistochemical staining was performed using a comprehensive panel of antibodies, including those directed against T-cell antigens, lineage associated transcription factors, immune checkpoint molecules, histone modifications and cytokine signaling molecules (*Online Supplementary methods*). The percentage of cells expressing nuclear T-bet and GATA3 was assessed in areas of dense lymphocytic infiltration determined by CD4 and CD8 staining. Cases with >50% cellular staining by both markers were deemed to co-express

T-bet and GATA3. For pSTAT3 and pSTAT5, >10% nuclear staining was considered positive. Flow cytometry was performed on cell suspensions prepared from tissue samples (*Online Supplementary methods*).

T-cell receptor gene rearrangement analysis

Polymerase chain reaction (PCR) analysis to determine clonal T-cell receptor beta (*TRB*) and/or gamma (*TRG*) gene rearrangement was performed using the 'Biomed-2' primers on DNA extracted from fresh or FFPE GI biopsies, lymph nodes, peripheral blood, and bone marrow mononuclear cells, as previously described[22].

Next-generation sequencing

Targeted next-generation sequencing of lesional and matched normal (control) tissue samples was performed using a custom panel of 465 cancer-associated genes, as previously described[23]. Variant calling required at least 5% variant allelic fraction (VAF) and at least 10 variant reads. Variants with an allele prevalence >0.01% in gnomAD, those reported as benign or likely benign in ClinVar, and germline variants present in the normal samples or inferred from VAFs were excluded from analysis. Non-synonymous variants that were not known driver mutations were analyzed by PolyPhen-2, SIFT, REVEL, and MetaSVM algorithms. Copy number changes were determined based on read depths using fragments per kilobase per million mapped reads (FPKM)[24] normalized to a pool of sex-matched control samples. The Fusion and Chromosomal Translocation Enumeration and Recovery Algorithm (FACTERA)[25] was used to detect structural chromosomal alterations, which were confirmed by PCR using breakpoint-

specific primers and Sanger sequencing of the PCR products (*Online Supplementary methods*).

Fluorescent In-situ hybridization (FISH) analysis

FISH analysis was performed to assess for *SETD2* and *JAK2* alterations on FFPE tissue sections using custom designed hybridization probes and dual-color break-apart probes (Oxford Gene Technologies Inc, Tarrytown, NY), respectively, as previously described[17,26]. Hybridization patterns of at least 100 tumor nuclei were reviewed for each probe. Cases were considered to have *SETD2* deletion, if the percentage of nuclei with *SETD2* locus deletion exceeded the cut-off value of 11.2%, and *JAK2* rearrangement, if the frequency of split-signals exceeded the cut-off value of 5.0%.

Results

Clinical characteristics and patient outcomes

Ten patients (M:F = 8:2) with ITLPD of the GI tract were identified at the contributing centers (cases 1, 2, and 4 were reported previously)[11]. The clinical features are summarized in Table 1. The median age at diagnosis was 45 years (range: 37-64 years). The ethnicity of 8 patients with available data was: White (n=5), Hispanic (n=2), and Asian (n=1). The most common signs and symptoms were diarrhea (70%), weight loss (60%), and abdominal pain (50%), with durations ranging from 2 to 16 years prior to diagnosis. Two patients lacked GI symptoms, with disease detected incidentally during routine colonoscopy and workup for inguinal lymphadenopathy. One patient had peptic ulcer disease, H. pylori infection and positive Hepatitis B and C serologies (case

9) and one (case 10) had a history of Crohn's disease. Five patients had been previously misdiagnosed as having celiac disease, seronegative and refractory to a gluten-free diet, and/or other types of lymphomas. The endoscopy findings included mucosal nodularity (70%), scalloping (40%), erythema (40%), decreased duodenal folds (30%), and polyps (20%). Common radiographic findings included abdominal lymphadenopathy (55%), bowel wall thickening (33%), and dilated bowel loops (33%). Biopsy-proven sites of disease included the small intestine (90%), colon (40%), stomach (30%), bone marrow (30%, one case only had cytogenetic evidence of disease), and inguinal lymph nodes (20%). Seven of 9 (77%) patients received therapeutic interventions consisting of steroids and/or chemotherapy; 2 were monitored expectantly. Six of 9 (66%) patients are alive with persistent disease and 3 (33%) died; one (case 5) due to septicemia and multiorgan failure following chemotherapy-induced intestinal perforation 1 year after diagnosis and 2 (cases 4 and 9) due to disease transformation 11 and 27 years post-diagnosis.

Morphologic features

All cases with small intestinal involvement displayed a dense diffuse or nodular infiltrate of small-sized lymphocytes in the lamina propria (Figures 1A and 2A), with extension into the submucosa noted in a subset. Villous atrophy was observed in 3/9 ITLPDs (cases 2, 4, 9; Figure 1B), however the villi were expanded (blunted appearance) (Figure 2B) in many cases, and all except one (case 10) showed crypt hyperplasia. The lymphocytes had round, ovoid or mildly irregular nuclei, variable fine or coarse chromatin, indistinct or small nucleoli, and scant or moderate cytoplasm (Figures 1C

and 2C). No significant increase in intraepithelial lymphocytes (IELs) was identified (Figures 1B and 2B), although focal lymphocytic infiltration of the epithelium was present in 4/9 ITLPDs (cases 1, 2, 4, and 7). Scattered lymphoid aggregates were seen in all except one ITLPD (case 5). Sparse, patchy mucosal infiltrates were noted in the 7 cases with gastric and/or colonic involvement. Mitotic figures and apoptotic cells were inconspicuous. No angiocentricity, angiodestruction, ulceration, or necrosis was observed. The histopathologic findings of the small intestinal biopsy from one patient with large cell transformation, available for review (case 4), were reported previously[11].

Immunophenotypic features

The immunophenotypic profiles of all cases are summarized in Table 2. Four of 10 (40%) ITLPDs were CD4+ (Figure 1D), 4 (40%) were CD8+ (Figure 2D) and one each (10%) was CD4+/CD8+ ("double-positive") and CD4-/CD8- ("double-negative"). All cases analyzed expressed CD2 (Figure 1E) and CD3 (Figures 1F and 2E). Other T-cell antigens were expressed by the majority (Figures 1G and 1H), variable downregulation or loss of CD5 and/or CD7 was seen in 4/10 cases (2/4 CD4+, 1/4 CD8+, and 1/1 double-negative). All except one CD8+ case and the CD4-/CD8- case displayed a cytotoxic immunophenotype, with TIA-1 expression (Figure 2F) noted in 3/4 cases and variable granzyme B (Figure 2G) expression observed in 2/4 CD8+ cases and in the CD4-/CD8- case. CD103 expression was detected in 2/4 CD8+ cases (Figure 2H), with one also showing partial CD56 expression (case 8) (Figure 2I). The CD4+/CD8+ and the CD4-/CD8- cases expressed PD-1. CD20 highlighted mucosal lymphoid follicles, but the neoplastic cells were CD20 negative in all ITLPDs. Surface TCRαβ expression was

observed in all cases evaluated by flow cytometry and none expressed TCRγδ. All analyzed cases were negative for BCL6, CD10, FoxP3, MATK, PD-L1 or CD30, however CD30 expression (and acquisition of cytotoxic proteins) was observed, and previously reported, upon large cell transformation (case 4)[11]. The Ki-67 proliferation index was low (<5%) in all ITLPDs evaluated (Figure 1J and 2J).

Cell of origin determination

Since a good correlation between the transcriptional profiles and immunohistochemistry for T-bet and GATA3 has been reported in T-cell lymphomas[27], we assessed T-bet and GATA3 expression by immunohistochemistry to determine the cell of origin of ITLPDs (Table 2, *Online Supplementary table 1,* and *Online Supplementary figure 1*). The CD4+ cases showed heterogeneity with regards to T-bet and GATA3 expression: 1 case each was T-bet+ and GATA3+, suggesting T-helper type 1 (Th1) and type 2 (Th2) lineage, respectively and 2 cases showed T-bet and GATA3 co-expression - hybrid Th1/Th2 profile (Figure 1K and 1L). The CD4+/CD8+ ITLPD also co-expressed T-bet and GATA3. The CD4-/CD8- and 3/4 (75%) CD8+ cases were GATA3 positive, implying a type-2-polarized effector T-cell (Tc2) phenotype and 1 CD8+ case showed T-bet and GATA3 co-expression (Figure 2K and 2L). Sequential analysis of 1 CD4+ ITLPD (case 2) showed a shift from a Th1/Th2 (T-bet and GATA3 co-expression) to Th2 (GATA3) phenotype over the course of disease. Double staining for T-bet and GATA3 performed in a subset (cases 2, 7, and 8) confirmed distinct T-bet and GATA3 positive as well as T-bet and GATA3 co-expressing lymphocytes (data not shown).

T-cell receptor gene rearrangement analysis

Clonal *TRB* and/or *TRG* rearrangement products were detected in all ITLPDs. In patients with longitudinal testing, similar sized peaks were observed in all samples, confirming persistence of the same lymphocytic clone.

Next-generation sequencing analysis

Targeted sequencing of 20 ITLPD biopsies from 10 patients and 7 matched normal samples (cases 1, 2, 4, 7-10) revealed 36 genetic variants, including 29 nonsynonymous single nucleotide variants, 1 small indel, and 6 structural variants. The average on-target coverage was 1059x (range 809x - 1639x). Twenty-three of 36 alterations were predicted to be pathogenic based on the published literature or prediction algorithms, the remaining 13 mutations were classified as variants of uncertain significance (*Online Supplementary table 2*).

The genetic alterations and their expected functional consequences are summarized in Table 3. Pathogenic or potentially pathogenic changes were identified in 8/10 (80%) ITLPDs. Three of 4 (75%) CD4+ cases and the CD4+/CD8+ and CD4-/CD8- cases harbored alterations of JAK-STAT signaling pathway genes. *STAT3* SH2 domain hotspot mutations (D661Y and S614R) were noted in three cases and one case each had a *SOCS1* deletion and a *STAT3-JAK2* rearrangement. Of note, conventional cytogenetic analysis had previously revealed a balanced translocation t(9;17)(p24;q21) in the latter case, the breakpoints corresponding to the *JAK2* and *STAT3* loci, and *JAK2* rearrangement was confirmed by FISH analysis. Concomitant mutations in epigenetic

modifier genes (*TET2*, *DNMT3A*, and *KMT2D*) were observed in 4 cases. A missense mutation in the cell cycle regulatory gene *CDKN2A* and a nonsense mutation in *TNFAIP3* was detected in 1 case each.

Two of the CD8+ ITLPDs exhibited structural chromosome alterations involving the interleukin-2 (*IL2*) gene. One case demonstrated an *IL2-RHOH* (Ras homolog family member H) rearrangement, representing an inversion of chromosome 4, with breakpoints occurring in the 3' untranslated region (3' UTR) of both *IL2* (chr4:123372863, c.*44) (Figure 3A) and *RHOH* (chr4:40246032, c.*449) genes. This rearrangement did not affect the coding sequence, but resulted in the deletion of a portion of the 3' UTR of *IL2*, including five of the six AU-rich regulatory elements (AREs, AUUUA). The "reciprocal" *RHOH-IL2* rearrangement had breakpoints in the 3' UTR of *RHOH* (chr4:40246006, c.*424) and intron 3 of *IL2* (chr4:123373085, c.352-67). Another CD8+ case demonstrated a 1.2 Mb deletion on chromosome 4q, beginning 5 base pairs downstream of the *IL2* stop codon (chr4:123372903, c.*5) (Figure 3D) and ending 6 kilobases upstream of TNFAIP3 interacting protein 3 (*TNIP3*) gene (chr4:122154953), deleting all regulatory elements from the *IL2* 3' UTR. In addition, an inversion, with breakpoints in exon 4 of *IL2* (chr4:123372912, c.457) and intron 2 of *TNIP3* (chr4:122128556, c.89+9014) was identified (Figure 3D). A missense mutation in the minichromosome maintenance complex component 5 (*MCM5*) gene was also identified in this case. The chromosome breakpoints were confirmed in all ITLPD samples with structural *IL2* alterations via PCR amplification and Sanger sequencing (Figures 3B-3C and 3E-3F). No pathogenic mutations or structural abnormalities were observed in two

CD8+ ITLPDs (cases 9 and 10), although a variant of uncertain significance was observed in one case (*Online Supplementary table 2*).

Longitudinal analysis of 5 ITLPDs (cases 1, 2, 4, 7, 8) revealed stable mutational profiles in 4 ITLPDs. Accrual of mutations over time was noted in 1 CD4+ ITLPD (case 4). Only a *KMT2D* frameshift mutation was detected in the first biopsy, obtained shortly after diagnosis. Additional mutations were identified at later time points, including a missense *TP53* mutation prior to disease transformation. Of interest, the first, second, and fourth time-point biopsies had shown different chromosome copy number changes (reported previously)[11], but none of the altered regions corresponded to the loci of mutated genes.

Evaluation of the SETD2-H3K36me3 axis

No *SETD2* mutations were observed by NGS analysis and FISH analysis did not detect any *SETD2* deletions in the cases analyzed. Additionally, no loss of SETD2 protein or H3K36me3 was detected by immunohistochemistry and H3K36me2 expression was observed in all analyzed cases (Figure 4A-4C, *Online Supplementary Table 3*).

Evaluation of JAK-STAT pathway activation

Due to the presence of frequent and recurrent genetic alterations targeting the *JAK-STAT* pathway and *IL2* genes, we evaluated pSTAT3-Y705 and pSTAT5-Y694 expression by immunohistochemistry to assess activation of the JAK-STAT signaling pathway. All 9 tested cases only showed single scattered or small clusters of nuclear

pSTAT3-Y705 and pSTAT5-Y694 positive cells (<10%) in all biopsies (Figure 4E-4F, *Online Supplementary Table 3*).

Discussion

Despite an increasing awareness of ITLPDs of the GI tract, deciphering their molecular pathogenesis and cellular origins has been challenging, in part due to the rarity of these disorders. In this study, comprising one of the largest series of cases evaluated, we delineate novel genetic alterations, including recurrent mutations and rearrangements, suggest cellular origins, and expand the immunophenotypic spectrum of these diseases.

The clinical presentations and disease course of our patients were largely congruent with previous descriptions[6,8–16]. Of interest, the ITLPDs were detected incidentally in two asymptomatic patients, which has rarely been documented[10]. A history of Crohn's disease has been reported in some patients with CD8+ ITLPDs[12,13], which was also the case for one patient in our series. Prior erroneous diagnoses of seronegative, refractory celiac disease in a high proportion (55%) of patients, were deemed to be the consequence of misinterpretation of the histopathologic changes and incomplete laboratory testing. Due to the relatively recent recognition of these disorders, it is not surprising that 40% of the ITLPDs in the current study had been previously misdiagnosed as aggressive intestinal T-cell lymphomas (EATL and MEITL). Extra-GI disease was observed more frequently (40%) in our series than previous reports, and transformation to aggressive lymphoma, which is considered rare[8,11,15,28], occurred in

two patients, including one with a CD8+ ITLPD. These findings emphasize the need for comprehensive clinical and laboratory evaluation and long-term follow-up of individuals with these disorders.

Next generation sequencing of the ITLPDs revealed genetic alterations in 80% of the cases, including mutations in JAK-STAT signaling pathway genes, observed in 75% of the CD4+ cases and in the CD4+/CD8+ and CD4-/CD8- cases. The *STAT3* D661Y and S614R mutations are well-characterized hotspot mutations that impart greater hydrophobicity to the SH2 dimerization surface and promote STAT3 nuclear localization and activation[29]. These mutations have been described in myriad lymphoid neoplasms and are quite frequent in T-large granular lymphocytic leukemia[29]. Perry et al. did not detect *STAT3* SH2 domain hotspot mutations in five cases analyzed by Sanger sequencing, although all tested cases were CD8+[12]. Deletion of *SOCS1*, a negative regulator of the JAK family proteins[30], which was seen in a colonic CD4+ ITLPD, is a recurrent abnormality in a variety of T-cell lymphomas and more commonly reported in mycosis fungoides[31]. We confirm the *STAT3-JAK2* rearrangement to be a recurrent event in CD4+ ITLPDs, however, this alteration was only observed in one (25%) of our cases compared to 4/5 (80%) cases in the series of Sharma et al[15].

Loss-of-function mutations in epigenetic modifier genes (*TET2*, *DNMT3A*, *KMT2D*) represented the next most commonly altered gene class, identified in 40% of cases and restricted to CD4+, CD4+/CD8+, and CD4-/CD8- cases. Mutations in epigenetic modifiers, which are believed to be early events in lymphomagenesis[32,33] and known to

cooperate with other mutations in fostering neoplastic transformation[33,34], have also been reported in diverse T-cell malignancies[33,35]. However, in contrast to other T-cell lymphomas[36], *IDH1/2* mutations were not observed in any ITLPD. Though not recurrent, mutations in *CDKN2A* and *TNFAIP3* suggest roles of cell cycle deregulation[37] and NF-κB activation[38] in the pathogenesis of at least some ITLPDs.

Structural chromosome alterations recurrently targeting the 3' UTR of the *IL2* gene that were identified in 50% of the CD8+ ITLPDs have not been described before. The rearrangements and deletions led to the loss of most or all of the regulatory AREs involved in mRNA stability. Studies in mitogen-stimulated Jurkat cells have shown that deletion of these regulatory elements, which act as binding sites for components of the mRNA degradation machinery[39], results in a longer half-life of *IL2* mRNA[40]. Whether these alterations lead to changes in the cellular localization of the *IL2* transcript or affect the assembly or composition of protein complexes that modulate activities beyond its 3' UTR-independent functions has not been investigated. An *IL2-TNFRSF17* rearrangement[41], resulting from t(4;16)(q26;p13)[41], was previously reported in a CD4+ ITLPD[9]. However, in contrast to our cases, the breakpoints in that case mapped to intron 3 of *IL2* and exon 1 of the B-cell maturation antigen (*BCMA*) gene, also known as tumor necrosis factor receptor superfamily member 17 (*TNFRSF17*)[41]. The authors detected a chimeric *IL2-TNFRSF17* mRNA, but no fusion protein was identified. The functional significance of the prior and current *IL2* alterations remains unknown.

Despite the frequent JAK-STAT pathway gene mutations and structural alteration of the *IL2* gene, which encodes a key T-cell cytokine that signals via the JAK-STAT pathway[42], none of the ITLPDs analyzed showed high-level pSTAT3 or pSTAT5 expression. Our findings are similar to Perry et al. who also did not observe significant pSTAT3 expression[12], but contrast with those of Sharma et al. who reported pSTAT5 expression in three of four cases with *STAT3-JAK2* rearrangements[15]. The reasons for the discrepant findings are unclear. It is plausible that the mutations simply augment the sensitivity of ITLPDs to cytokine stimulation, enhancing ligand-mediated signaling as described in other T-cell lymphomas[43] and aberrant IEL proliferations in refractory celiac disease type 2[44] that harbor *STAT3* mutations.

On analysis of serial samples, acquisition of additional mutations, including those targeting genes involved in the DNA damage response (*TP53*, *POLE*) were only identified in an ITLPD that transformed to aggressive lymphoma. It is possible that ineffective DNA repair mechanisms fueled acquisition of additional mutations and complex chromosome changes in this case[11]. It is unclear if prolonged azathioprine therapy played a role in genomic evolution. Nonetheless, this and other cases in our series as well as those published previously highlight the futility of genotoxic chemotherapeutic agents for treating ITLPDs of the GI tract. The prognostic relevance of periodic genetic analysis needs to be assessed in future larger studies.

Our findings indicate that ITLPDs of the GI tract share certain pathogenetic mechanisms with other intestinal T-cell lymphomas. Similar to our cohort, mutations in the JAK-STAT

pathway genes represent the most frequent alterations in EATL, MEITL, and intestinal T-cell lymphoma, NOS[17–21]. Similarly, loss-of-function mutations in epigenetic modifier genes and DNA damage repair genes have also been reported in aggressive intestinal T-cell lymphomas[17,18]. In contrast to EATL and MEITL, however, *SETD2* mutations or deletions were not seen in any ITLPD and the burden of pathogenic alterations in ITLPDs appears lower[17,18].

ITLPDs of the GI tract are immunophenotypically heterogeneous diseases. Our study revealed a few unique features that are worth highlighting. In addition to CD4+, CD8+, and CD4-/CD8- ITLPDs, we describe a CD4+/CD8+ (double-positive) case. Two ITLPDs with a similar phenotype were recently reported from the US and China[15,45]. Two of our CD8+ ITLPDs expressed CD103, which has not been documented before. Prior sporadic cases of CD103+ ITLPDs have all been of CD4 T-cell lineage[10,13]. These ITLPDs could arise from αE integrin expressing lamina propria T-cells[46], but the possibility of activation induced upregulation of CD103 cannot be excluded[47,48]. Of note, one CD103+ CD8+ ITLPD also showed focal CD56 expression. Distinguishing such cases from MEITL can be challenging, however, in addition to the clinical presentation and course, the presence of small lymphocytes with bland cytomorphology confined to the lamina propria, absent MATK expression, and a low Ki-67 index, can help establish a diagnosis of ITLPD. Evaluation of SETD2 and H3K36me3 expression can also aid in differentiating ITLPDs from MEITL, which frequently show loss of SETD2 and H3K36 trimethylation[17].

ITLPDs of the GI tract are thought to originate from mucosal T-cells, but the cell of origin of different disease subsets has not been clarified. Absence of FoxP3 and T-follicular helper (TFH) cell markers in the current and previously reported CD4+ ITLPDs[11,16] argues against their derivation from regulatory T-cells or TFH cells. Based on expression of T-bet and GATA3, which are transcription factors regulating CD4+ Th1 vs. Th2 cell fate decisions, the CD4+ and CD4+/CD8+ ITLPDs in our series displayed Th1, Th2, or hybrid Th1/2 profiles. It is not known if ITLPDs with the latter profile develop directly from naïve T-cells into bifunctional mucosal Th1/2 cells, similar to those described in primary immune responses against parasites, which help dampen inflammation[49], or derive from Th1 or Th2 cells that have undergone cytokine mediated reprogramming to acquire a Th1/Th2 phenotype, with concomitant production of Th1 and Th2 cytokines[50]. The phenotypic shift from a Th1/Th2 to Th2 profile over time, observed in one CD4+ case, suggests lineage (and possibly functional) plasticity of at least a subset of ITLPDs. The majority of the CD8+ cases and the CD4-/CD8- ITLPD displayed a Tc2 phenotype[51]. Besides orchestrating diverse functions in CD4+ T-helper cells, GATA3 also regulates the activation, homeostasis, and cytolytic activity of CD8+ T-cells[52]. The significance of T-bet/GATA3 co-expression in CD8+ ITLPDs is unknown. It must be pointed out that despite the reported concordance between the transcriptional and protein expression profiles of T-bet and GATA3 in certain T-cell lymphomas[27], the definitive lineage (and function) of neoplastic T-cells cannot be ascertained based on the expression of single lineage-associated transcription factors. Cytokine profiling and in vitro functional studies are awaited for confirmation of our observations. Contrary to

observations in PTCL, NOS[27,53,54], however, an inferior prognostic impact of GATA3 expression was not apparent in our series of ITLPDs.

In conclusion, our study reveals considerable immunophenotypic and genetic heterogeneity of GI ITLPDs. We describe recurrent and novel genetic abnormalities in different immunophenotypic subtypes of GI ITLPDs that implicate deregulated cytokine signaling and epigenetic alterations in disease pathogenesis. It is hoped that future unbiased interrogation of ITLPD genomes and transcriptomes as well as mechanistic studies will help clarify the cell of origin and the functional consequences of the underlying genetic aberrations in these rare disorders, opening the door for targeted, less toxic and more effective therapies.

1. Swerdlow S, Campo E, Harris N, et al., editors. World Health Organization Classification of Tumours of Haematopoietic and Lymphoid Tissues. Lyon, France: IARC; 2016.
2. Foukas PG, de Leval L. Recent advances in intestinal lymphomas. Histopathology. 2015;66(1):112-136.
3. Wu XC, Andrews P, Chen VW, Groves FD. Incidence of extranodal non-Hodgkin lymphomas among whites, blacks, and Asians/Pacific Islanders in the United States: Anatomic site and histology differences. Cancer Epidemiol. 2009;33(5):337-346.
4. Delabie J, Holte H, Vose JM, et al. Enteropathy-associated T-cell lymphoma:

clinical and histological findings from the International Peripheral T-Cell Lymphoma Project. Blood. 2011;118(1):148-156.

5. Tan SY, Chuang SS, Tang T, et al. Type II EATL (epitheliotropic intestinal T-cell lymphoma): a neoplasm of intra-epithelial T-cells with predominant CD8αα phenotype. Leukemia. 2013;27(8):1688-1696.
6. Matnani R, Ganapathi KA, Lewis SK, Green PH, Alobeid B, Bhagat G. Indolent T- and NK-cell lymphoproliferative disorders of the gastrointestinal tract: a review and update. Hematol Oncol. 2017;35(1):3-16.
7. Xia D, Morgan EA, Berger D, Pinkus GS, Ferry JA, Zukerberg LR. NK-Cell Enteropathy and Similar Indolent Lymphoproliferative Disorders. Am J Clin Pathol. 2018;151(1):75-85.
8. Carbonnel F, D'Almagne H, Lavergne A, et al. The clinicopathological features of extensive small intestinal CD4 T cell infiltration. Gut. 1999;45(5):662-667.
9. Carbonnel F, Lavergne A, Messing B, et al. Extensive small intestinal T-cell lymphoma of low-grade malignancy associated with a new chromosomal translocation. Cancer.1994;73(4):1286-1291.
10. Hirakawa K, Fuchigami T, Nakamura S, et al. Primary gastrointestinal T-cell lymphoma resembling multiple lymphomatous polyposis. Gastroenterology. 1996;111(3):778-782.
11. Margolskee E, Jobanputra V, Lewis SK, Alobeid B, Green PH, Bhagat G. Indolent Small Intestinal CD4+ T-cell Lymphoma Is a Distinct Entity with Unique Biologic and Clinical Features. PLoS One. 2013;8(7):e68343.
12. Perry AM, Warnke RA, Hu Q, et al. Indolent T-cell lymphoproliferative disease of

the gastrointestinal tract. Blood. 2013;122(22):3599-3606.

13. Malamut G, Meresse B, Kaltenbach S, et al. Small Intestinal CD4+ T-Cell Lymphoma Is a Heterogenous Entity With Common Pathology Features. Clin Gastroenterol Hepatol. 2014;12(4):599-608.
14. Edison N, Belhanes-Peled H, Eitan Y, et al. Indolent T-cell lymphoproliferative disease of the gastrointestinal tract after treatment with adalimumab in resistant Crohn's colitis. Hum Pathol. 2016;5745-50.
15. Sharma A, Oishi N, Boddicker RL, et al. Recurrent STAT3-JAK2 fusions in indolent T-cell lymphoproliferative disorder of the gastrointestinal tract. Blood. 2018;131(20):2262.
16. Sena Teixeira Mendes L, Attygalle AD, Cunningham D, et al. CD4-positive small T-cell lymphoma of the intestine presenting with severe bile-acid malabsorption: A supportive symptom control approach. Br J Haematol. 2014;167(2):265-269.
17. Roberti A, Dobay MP, Bisig B, et al. Type II enteropathy-associated T-cell lymphoma features a unique genomic profile with highly recurrent SETD2 alterations. Nat Commun. 2016;(7):12602.
18. Moffitt AB, Ondrejka SL, McKinney M, et al. Enteropathy-associated T cell lymphoma subtypes are characterized by loss of function of SETD2. J Exp Med. 2017;214(5):1371-1386.
19. Nairismägi ML, Tan J, Lim JQ, et al. JAK-STAT and G-protein-coupled receptor signaling pathways are frequently altered in epitheliotropic intestinal T-cell lymphoma. Leukemia. 2016;30(6):1311-1319.
20. Küçük C, Jiang B, Hu X, et al. Activating mutations of STAT5B and STAT3 in

lymphomas derived from γδ-T or NK cells. Nat Commun. 2015;(6):6025.

21. Nicolae A, Xi L, Pham TH, et al. Mutations in the JAK/STAT and RAS signaling pathways are common in intestinal T-cell lymphomas. Leukemia. 2016;30(11):2245-2247.

22. van Dongen JJM, Langerak AW, Brüggemann M, et al. Design and standardization of PCR primers and protocols for detection of clonal immunoglobulin and T-cell receptor gene recombinations in suspect lymphoproliferations: Report of the BIOMED-2 Concerted Action BMH4-CT98-3936. Leukemia. 2003;17(12):2257-2317.

23. Margolskee E, Jobanputra V, Jain P, et al. Genetic landscape of T- and NK-cell post-transplant lymphoproliferative disorders. Oncotarget. 2016;7(25):37636-37648.

24. Trapnell C, Williams BA, Pertea G, et al. Transcript assembly and quantification by RNA-Seq reveals unannotated transcripts and isoform switching during cell differentiation. Nat Biotechnol. 2010;28(5):511-515.

25. Newman AM, Bratman S V., Stehr H, et al. FACTERA: a practical method for the discovery of genomic rearrangements at breakpoint resolution. Bioinformatics. 2014;30(23):3390-3393.

26. Tang G, Sydney Sir Philip JK, Weinberg O, et al. Hematopoietic neoplasms with 9p24/JAK2 rearrangement: a multicenter study. Mod Pathol 2019;32(4):490-498.

27. Iqbal J, Wright G, Wang C, et al. Gene expression signatures delineate biologic and prognostic subgroups in peripheral T-cell lymphoma. Blood. 2014;123(19):2915-2924.

28. Perry AM, Bailey NG, Bonnett M, Jaffe ES, Chan WC. Disease Progression in a Patient With Indolent T-Cell Lymphoproliferative Disease of the Gastrointestinal Tract. Int J Surg Pathol. 2019;27(1):102-107.
29. Koskela HLM, Eldfors S, Ellonen P, et al. Somatic STAT3 mutations in large granular lymphocytic leukemia. N Engl J Med. 2012;366(20):1905-1913.
30. Liau NPD, Laktyushin A, Lucet IS, et al. The molecular basis of JAK/STAT inhibition by SOCS1. Nat Commun. 2018;9(1):1558.
31. Bastidas Torres AN, Cats D, Mei H, et al. Genomic analysis reveals recurrent deletion of JAK-STAT signaling inhibitors HNRNPK and SOCS1 in mycosis fungoides. Genes Chromosom Cancer. 2018;57(12):653-664.
32. Schwartz FH, Cai Q, Fellmann E, et al. TET2 mutations in B cells of patients affected by angioimmunoblastic T-cell lymphoma. J Pathol. 2017;242(2):129-133.
33. Van Arnam JS, Lim MS, Elenitoba-Johnson KSJ. Novel insights into the pathogenesis of T-cell lymphomas. Blood. 2018;131(21):2320-2330.
34. Zang S, Li J, Yang H, et al. Mutations in 5-methylcytosine oxidase TET2 and RhoA cooperatively disrupt T cell homeostasis. J Clin Invest. 2017;127(8):2998-3012.
35. Watatani Y, Sato Y, Miyoshi H, et al. Molecular heterogeneity in peripheral T-cell lymphoma, not otherwise specified revealed by comprehensive genetic profiling. Leukemia. 2019 May 15. [Epub ahead of print]
36. Cairns RA, Iqbal J, Lemonnier F, et al. IDH2 mutations are frequent in angioimmunoblastic T-cell lymphoma. Blood. 2012;119(8):1901-1903.
37. Foulkes WD, Flanders TY, Pollock PM, Hayward NK. The CDKN2A (p16) Gene

and Human Cancer. Mol Med. 1997;3(1):5-20.

38. Wenzl K, Manske MK, Sarangi V, et al. Loss of TNFAIP3 enhances MYD88L265P-driven signaling in non-Hodgkin lymphoma. Blood Cancer J. 2018;8(10):97.

39. Myer VE, Fan XC, Steitz JA. Identification of HuR as a protein implicated in AUUUA-mediated mRNA decay. EMBO J. 1997;16(8):2130-2139.

40. Chen CY, Del Gatto-Konczak F, Wu Z, Karin M. Stabilization of interleukin-2 mRNA by the c-Jun NH2-terminal kinase pathway. Science. 1998;280(5371):1945-1949.

41. Laâbi Y, Gras MP, Carbonnel F, et al. A new gene, BCM, on chromosome 16 is fused to the interleukin 2 gene by a t(4;16)(q26;p13) translocation in a malignant T cell lymphoma. EMBO J. 1992;11(11):3897-3904.

42. Ross SH, Cantrell DA. Signaling and Function of Interleukin-2 in T Lymphocytes. Annu Rev Immunol. 2018;36(1):411-433.

43. Chen J, Zhang Y, Petrus MN, et al. Cytokine receptor signaling is required for the survival of ALK- anaplastic large cell lymphoma, even in the presence of JAK1/STAT3 mutations. Proc Natl Acad Sci U S A. 2017;114(15):3975-3980.

44. Ettersperger J, Montcuquet N, Malamut G, et al. Interleukin-15-Dependent T-Cell-like Innate Intraepithelial Lymphocytes Develop in the Intestine and Transform into Lymphomas in Celiac Disease. Immunity. 2016;45(3):610-625.

45. Guo L, Wen Z, Su X, Xiao S, Wang Y. Indolent T-cell lymphoproliferative disease with synchronous diffuse large B-cell lymphoma. Medicine (Baltimore). 2019;98(17):e15323.

46. Farstad IN, Halstensen TS, Lien B, Kilshaw PJ, Lazarovitz AI, Brandtzaeg P. Distribution of β7 integrins in human intestinal mucosa and organized gut-associated lymphoid tissue. Immunology. 1996;89(2):227-237.
47. Micklem KJ, Dong Y, Willis A, et al. HML-1 antigen on mucosa-associated T cells, activated cells, and hairy leukemic cells is a new integrin containing the beta 7 subunit. Am J Pathol. 1991;139(6):1297-301.
48. Shaw SK, Brenner MB. The β 7 integrins in mucosal homing and retention. Semin Immunol. 1995;7(5):335-342.
49. Peine M, Rausch S, Helmstetter C, et al. Stable T-bet+GATA-3+ Th1/Th2 Hybrid Cells Arise In Vivo, Can Develop Directly from Naive Precursors, and Limit Immunopathologic Inflammation. PLoS Biol. 2013;11(8):e1001633.
50. Hegazy AN, Peine M, Helmstetter C, et al. Interferons Direct Th2 Cell Reprogramming to Generate a Stable GATA-3+T-bet+ Cell Subset with Combined Th2 and Th1 Cell Functions. Immunity. 2010;32(1):116-128.
51. Fox A, Harland KL, Kedzierska K, Kelso A. Exposure of human CD8+ T cells to type-2 cytokines impairs division and differentiation and induces limited polarization. Front Immunol. 2018;9:1141.
52. Tai TS, Pai SY, Ho IC. GATA-3 Regulates the Homeostasis and Activation of CD8+ T Cells. J Immunol. 2013;190(1):428-437.
53. Wang T, Feldman AL, Wada DA, et al. GATA-3 expression identifies a high-risk subset of PTCL, NOS with distinct molecular and clinical features. Blood. 2014;123(19):3007-3015.
54. Manso R, Bellas C, Martín-Acosta P, et al. C-MYC is related to GATA3

expression and associated with poor prognosis in nodal peripheral T-cell lymphomas. Haematologica. 2016;101(8):e336-338.

Case	Age	Sex	Eth	Presenting signs & symptoms	Duration of symptoms prior to diagnosis (years)	Other conditions	Prior diagnosis	Endoscopic findings	Radiographic findings	Sites of involvement†	Ann Arbor stage (at diagnosis)	Treatment	Outcome (Cause of death)
1*	53	M	W	Diarrhea, weight loss, night sweats	16	None	Celiac disease	Mucosal nodularity, scalloping, decreased duodenal folds, erythema	Mild mesenteric LAD, mild FDG activity	Duodenum, jejunum, ileum	IEB	Bud	AWD, 9 years
2*	50	F	W	Diarrhea, weight loss, abd pain, fatigue	3	None	Celiac disease	Mucosal nodularity, Scalloping	SB wall thickening and dilation	Duodenum, ileum, appendix, colon, stomach, BM‡	IEB	Pral, Romi, Bud	AWD, 7 years
3	64	F	NA	No GI symptoms	0	NA	None	Sessile polyp in colon	NA	Colon	NA	NA	NA
4*†	37	M	W	Diarrhea, weight loss	2	None	Celiac disease	Mucosal nodularity, Scalloping	Normal	Duodenum, ileum, colon, stomach	IEB	Bud, Pred, Aza	D, 11 years (Large cell trans)
5	62	M	H	Diarrhea weight loss	NA	NA	Celiac disease, EATL	Mucosal nodularity, scalloping, mosaic pattern, increased vascularity, ulcer	SB and LB dilation	Duodenum, jejunum, inguinal LN	IEB	CP, Dox, VCR, Pred	D, 1 year (SB perf)
6	41	M	NA	No GI symptoms	0	MG	None	Polypoid ileal lesions	Mesenteric and iliac LAD	Ileum, colon, stomach, inguinal LN, BM	IVE	None	AWD, 1 year
7	38	M	W	Diarrhea, abd pain, vomiting	5	Lyme disease	EATL	Mucosal nodularity, decreased duodenal folds, gastric erythema	SB wall thickening, intuss, mesenteric LAD	Duodenum, jejunum, ileum, colon	IE	None	AWD, 21 years
8	38	M	H	Diarrhea, weight loss, abd pain	5	CHD	MEITL	Mucosal nodularity, erythema, friability	Mesenteric and retroperitoneal LAD, incr FDG activity	Duodenum, ileum, colon	IEB	CP, Dox, VCR, Bud, Pred, Etop, AGS67E	AWD, 7 years
9†	41	M	A	Abd pain	3	PUD, H. pylori, viral hep (B & C)	Atyp lymphoid infiltrate, favor MZL	Mucosal nodularity, decreased duodenal folds	Abd LAD, mild FDG activity, splenomegaly	Duodenum, stomach, BM	IE	IFN, CP, Dox, VCR, Pred, Gem	D, 27 years (Large cell trans)
10	49	M	W	Diarrhea weight loss, abd pain	5	Crohn's disease§	Celiac disease, EATL	Flattened SB mucosa, gastric erythema	Mild SB wall thickening and dilation, partial SB obstruction	Duodenum, jejunum	IEB	CP, Dox, VCR, Pred, Mes, Aza	AWD, 19 years

Table 1: Clinical characteristics of gastrointestinal ITLPD patients
A, Asian; abd, abdominal; AGS67E, Anti-CD37 monoclonal antibody AGS67E; AWD, alive with disease; Aza, Azathioprine; BM, bone marrow; Bud, budesonide; CHD, congenital heart disease; CP, cyclophosphamide; D, dead; Dox, doxorubicin; EATL, enteropathy associated T-cell lymphoma; Eth, ethnicity; Etop, Etoposide; F, female; FDG, fluorodeoxyglucose; Gem, Gemcitabine; GI, gastrointestinal; H, Hispanic; hep, hepatitis; IFN, Interferon; incr, increased; intuss, intussusception; LAD, lymphadenopathy; LB, large bowel; LN, lymph node; M, male; MEITL, monomorphic epitheliotropic intestinal T-cell lymphoma; Mes, mesalamine; MG, monoclonal gammopathy; MZL, marginal zone lymphoma; NA, not available; perf, perforation; PUD, peptic ulcer disease; Pral, Pralatrexate; Pred, Prednisone; Romi, Romidepsin; SB, small bowel; trans, transformation; VCR; vincristine; W, White
*Previously published cases.
†Findings prior to large cell transformation.
‡ Bone marrow involvement was detected by cytogenetic analysis; there was no morphologic or immunophenotypic evidence of disease and TCRβ PCR showed polyclonal products.
§ Biopsies diagnosed as Crohn's disease were not reviewed by authors.

Case	CD4	CD8	CD2	CD3	CD5	CD7	TIA-1	GrzB	Perf	CD103	CD56	BCL6	CD10	PD-1	PD-L1	FoxP3	MATK	TCRαβ	TCRγδ	CD30	Ki67 (%)	T-bet	GATA3
1*	+	-	+	+	-/+	-	-	-	-	-	-	-	-	-	-	-	-	+	-	-	<5	+	-
2*	+	-	+	+	+	+	-	-	-	-	-	-	-	-	-	-	-	+	-	-	<5	+	+
3	+	-	NA	+	+	+	-	-	-	-	-	NA	NA	NA	-	NA	-	+	-	-	NA	-	+
4*†	+	-	+	+	+/-	-	-	-	-	-	-	-	-	-	-	-	-	+/-	-	-	<5	+	+
5	+	+	+	+	+	+	-	-	-	-	-	-	-	+	-	-	-	+	-	-	<5	+	+
6	-	-	+	+	+	-/+	+	-/+	NA	-	-	-	-	+	NA	-	NA	+	-	-	<5	-	+
7	-	+	+	+	+	+	-	-	-	+	-	-	-	-	-	-	-	+	-	-	<5	-	+
8	-	+	+	+	+	+	+	+/-	-	+	+/-	-	-	-	-	-	-	+	-	-	<5	+	+
9†	-	+	+	+	-	-/+	+	-	-	-	-	-	-	-	-	-	-	+	-	-	<5	-	+
10	-	+	+	+	+	+	+	+	-	-	-	-	-	-	-	-	NA	+	-	-	<5	-	+
TOTAL	5/10 (50%)	4/10 (40%)	9/9 (100%)	10/10 (100%)	8/10 (80%)	6/10 (60%)	4/10 (40%)	2/9 (22%)	0/9 (0%)	2/10 (20%)	1/10 (10%)	0/9 (0%)	0/9 (0%)	2/9 (22%)	0/9 (0%)	0/9 (0%)	0/8 (0%)	10/10 (100%)	0/10 (0%)	0/10 (0%)		5/10 (50%)	9/10 (90%)
CD4+	4/4 (100%)	0/4 (0%)	3/3 (100%)	4/4 (100%)	3/4 (75%)	2/4 (50%)	0/4 (0%)	0/4 (0%)	0/4 (0%)	0/4 (0%)	0/4 (0%)	0/3 (0%)	0/3 (0%)	0/3 (0%)	0/4 (0%)	0/3 (0%)	0/4 (0%)	4/4 (100%)	0/4 (0%)	0/4 (0%)		3/4 (75%)	3/4 (75%)
DP	1/1 (100%)	1/1 (100%)	1/1 (100%)	1/1 (100%)	1/1 (100%)	1/1 (100%)	0/1 (0%)	0/1 (0%)	0/1 (0%)	0/1 (0%)	0/1 (0%)	0/1 (0%)	0/1 (0%)	1/1 (100%)	0/1 (0%)	0/1 (0%)	0/1 (0%)	1/1 (100%)	0/1 (0%)	0/1 (0%)		1/1 (100%)	1/1 (100%)
DN	0/1 (0%)	0/1 (0%)	1/1 (100%)	1/1 (100%)	1/1 (100%)	0/1 (0%)	1/1 (100%)	0/1 (0%)	NA	0/1 (0%)	0/1 (0%)	0/1 (0%)	0/1 (0%)	1/1 (100%)	NA	0/1 (0%)	NA	1/1 (100%)	0/1 (0%)	0/1 (0%)		0/1 (0%)	1/1 (100%)
CD8+	0/4 (0%)	4/4 (100%)	4/4 (100%)	4/4 (100%)	3/4 (75%)	3/4 (75%)	3/4 (75%)	2/4 (50%)	0/4 (0%)	2/4 (50%)	1/4 (25%)	0/4 (0%)	0/4 (0%)	0/4 (0%)	0/4 (0%)	0/4 (0%)	0/3 (0%)	4/4 (100%)	0/4 (0%)	0/4 (0%)		1/4 (25%)	4/4 (100%)

Table 2: Immunophenotypic characteristics of gastrointestinal ITLPDs
+, positive; -, negative; DN, double-negative; DP, double-positive; GrzB, Granzyme B; NA, not available; Perf, perforin; TCRαβ, T-cell receptor alpha-beta; TCRγδ, T-cell receptor gamma-delta
*Previously published cases
†Findings at diagnosis prior to large cell transformation

Case	*Phenotype*	*Time Point (years following diagnosis)*	*Genetic alterations*	*Predicted Functional Consequence*
1	**CD4+**	2.5	*STAT3* (c.1981G>T, p. D661Y) *TET2* (c.2457T>G, p. Y819*)	Activation of JAK-STAT pathway Altered DNA methylation
		7.9	*STAT3* (c.1981G>T, p. D661Y) *TET2* (c.2457T>G, p. Y819*)	Activation of JAK-STAT pathway Altered DNA methylation
2	**CD4+**	0	*STAT3-JAK2* rearrangement *TNFAIP3* (c.857T>G, p.L286*)	Activation of JAK-STAT pathway Activation of NF-κB pathway
		2.2	*STAT3-JAK2* rearrangement *TNFAIP3* (c.857T>G, p.L286*)	Activation of JAK-STAT pathway Activation of NF-κB pathway
		6.4	*STAT3-JAK2* rearrangement *TNFAIP3* (c.857T>G, p.L286*)	Activation of JAK-STAT pathway Activation of NF-κB pathway
3	**CD4+**	0	*SOCS1* deletion	Activation of JAK-STAT pathway
4	**CD4+**	0.5	*KMT2D* (c.13105_13108del, p.L4369fs)	Altered histone modification
		7.4	*KMT2D* (c.13105_13108del, p.L4369fs) *DIS3* (c.1115T>C, p.L372P)	Altered histone modification Altered RNA processing and decay
		11.5	*KMT2D* (c.13105_13108del, p.L4369fs) *DIS3* (c.1115T>C, p.L372P) *MAPK1* (c.965A>T, p.E322V) *TP53* (c.743G>A, p.R248Q) *POLE* (c.4090C>T, p.R1364C)	Altered histone modification Altered RNA processing and decay Activation of RAS-RAF-MAPK pathway DNA repair/ cell cycle dysregulation Altered DNA repair and replication
		11.7†	*KMT2D* (c.13105_13108del, p.L4369fs) *DIS3* (c.1115T>C, p.L372P) *MAPK1* (c.965A>T, p.E322V) *TP53* (c.743G>A, p.R248Q) *POLE* (c.4090C>T, p.R1364C) *TET2* (c.2725C>T, p.Q909*) *SMAD4* (c.404G>A, p.R135Q) *SF3B1* (c.2584G>A, p.E862K)	Altered histone modification Altered RNA processing and decay Activation of RAS-RAF-MAPK pathway DNA repair/ cell cycle dysregulation Altered DNA repair and replication Altered DNA methylation Activation of TGF-β pathway Altered RNA splicing
5	**CD4+/CD8+**	0	*STAT3* (c.1842C>G, p.S614R) *DNMT3A* (c.2116G>T, p.G706W) *CDKN2A* (c.322G>A, p.D108N)	Activation of JAK-STAT pathway Altered DNA methylation Cell cycle checkpoint (G1-to-S) dysregulation
6	**CD4-/CD8-**	0	*STAT3* (c.1840A>C, p.S614R) *KMT2D* (c.9415C>G, p.P3139A)	Activation of JAK-STAT pathway Altered histone modification
7	**CD8+**	0	*IL2-RHOH* rearrangement‡	Unknown
		3.9	*IL2-RHOH* rearrangement‡	Unknown
		6.1	*IL2-RHOH* rearrangement‡	Unknown
8	**CD8+**	0	*IL2* 3' UTR deletion‡, *IL2-TNIP3* rearrangement‡ *MCM5* (c.2080A>T, p.I694F)	Unknown Cell cycle dysregulation
		4.3	*IL2* 3' UTR deletion‡, *IL2-TNIP3* rearrangement‡ *MCM5* (c.2080A>T, p.I694F)	Unknown Cell cycle dysregulation
		6.4	*IL2* 3' UTR deletion‡, *IL2-TNIP3* rearrangement‡ *MCM5* (c.2080A>T, p.I694F)	Unknown Cell cycle dysregulation
9	**CD8+**	14	None identified	NA
10	**CD8+**	10.8	None identified	NA

Table 3: Genetic alterations in gastrointestinal ITLPDs
NA, not applicable
† Large cell transformation
‡ Confirmed by breakpoint specific PCR and Sanger sequencing

Figure Legends

Figure 1 - Morphologic and immunophenotypic features of CD4+ ITLPD of the GI tract.

(A) A duodenal biopsy (case 2) shows a dense lymphocytic infiltrate within the lamina propria, as well as villous atrophy and crypt hyperplasia. **(B)** There is no increase in intraepithelial lymphocytes. **(C)** The lymphocytes are small and have round to ovoid nuclei, fine chromatin, indistinct or small nucleoli, and moderate pale pink cytoplasm. The lymphocytes express **(D)** CD4, **(E)** CD2, **(F)** CD3, **(G)** CD5, and **(H)** CD7. **(I)** The neoplastic cells do not express CD103. **(J)** The Ki-67 proliferation index is low (<5%). The majority of cells are **(K)** T-bet+, however, 50% also express **(L)** GATA3.

Figure 2 - Morphologic and immunophenotypic features of CD8+ ITLPD of the GI tract.

(A) An ileal biopsy (case 8) shows a dense mucosal lymphocytic infiltrate expanding the lamina propria and widening the villi, no villous atrophy is present but the crypts are hyperplastic. **(B)** Small clusters of lymphocytes are seen within the villus epithelium along the lateral edges, there is no increase in intraepithelial lymphocytes. **(C)** The lymphocytes are small and have round or oval nuclei, condensed chromatin, indistinct nucleoli, and scant to moderate clear or pale pink cytoplasm. The lymphocytes express **(D)** CD8 and **(E)** CD3. Most of the cells express the cytotoxic marker **(F)** TIA1 and **(G)** Granzyme B is expressed by a subset. **(H)** The lymphocytes are CD103+ and a subset expresses **(I)** CD56. **(J)** The Ki-67 proliferation index is low (<5%). The majority of cells express **(K)** GATA3, but 60% also show **(L)** T-bet expression.

Figure 3: Structural chromosome alterations of the *IL2* gene in CD8+ ITLPDs

In case 7, **(A)** two chromosome breaks were detected as a consequence of a rearrangement involving the 3' UTR of *IL2* and 3' UTR of *RHOH* ("*IL2-RHOH*") and a reciprocal rearrangement involving intron 3 of *IL2* and the 3' UTR of *RHOH* ("*RHOH-IL2*"). **(B)** Pile-up of a subset of reads

mapping to the *IL2-RHOH* rearrangement. **(C)** Sanger sequencing validation of the fusion breakpoints.

In case 8, **(D)** two chromosome breaks were observed due to a 1.2 Mb deletion spanning the majority of the 3' UTR of *IL2* and a portion of the intergenic region between *IL2* and *TNIP3 ("IL2 3' UTR del")* and an inversion involving exon 4 of *IL2* and intron 2 of *TNIP3 ("IL2-TNIP3")*. **(E)** Pile-up of a subset of reads mapping to the *IL2* 3' UTR deletion. **(F)** Sanger sequencing validation of the deletion breakpoints.

† Chromosome position based on assembly GRCh37.p13

Figure 4: Analysis of the SETD2-H3K36me3 axis and JAK-STAT pathway activation. IHC analysis of a CD4+ ITLPD with *STAT3-JAK2* rearrangement (case 2) shows preserved **(A)** SETD2, **(B)** H3K36me2, and **(C)** H3K36me3 protein expression. The lymphocytes express **(D)** CD4. Only a few scattered **(E)** pSTAT3-Y705 positive and **(F)** pSTAT5-Y694 positive cells are noted (comprising <10% of the neoplastic lymphocytes).

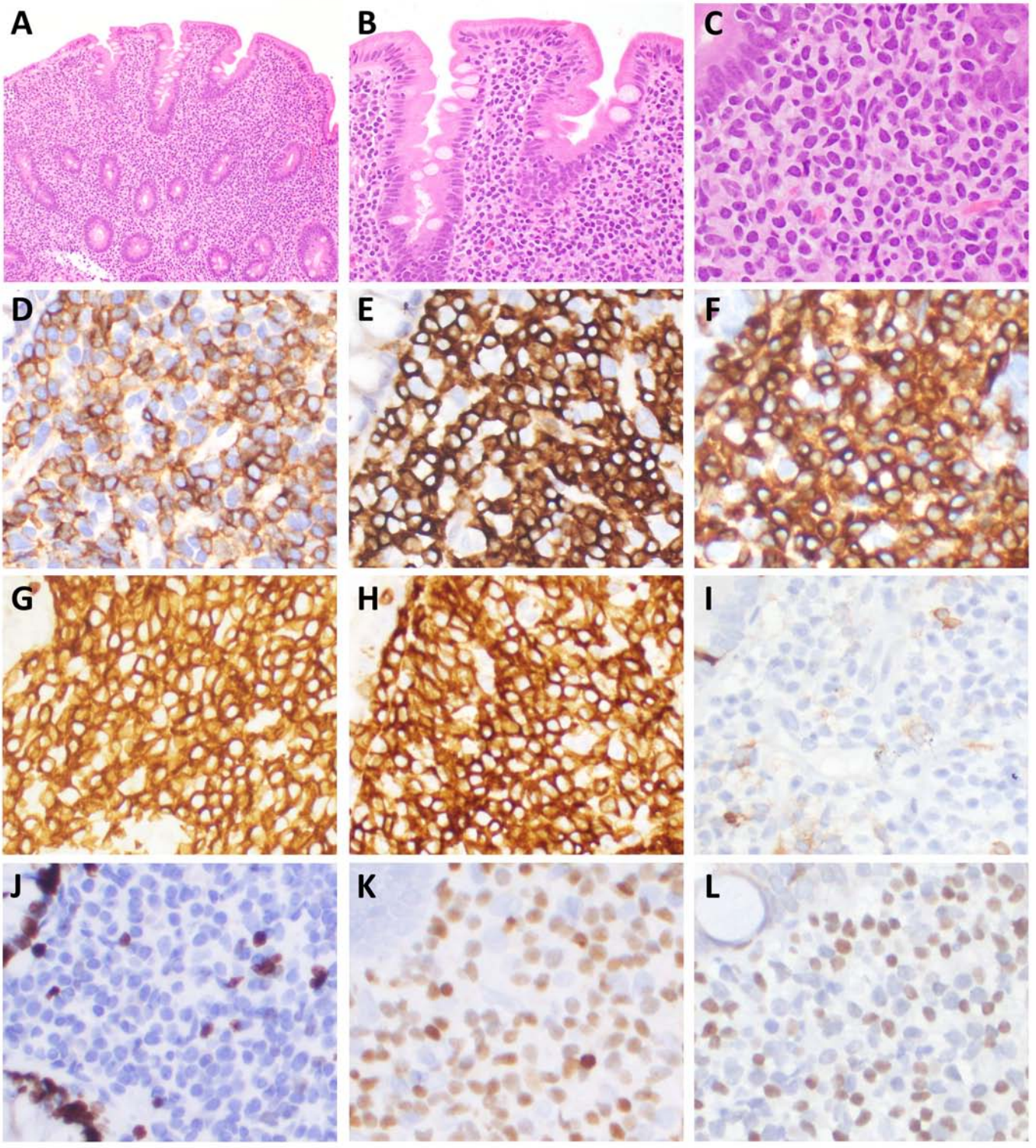
A
B
C
D
E
F
G
H
I
J
K
L

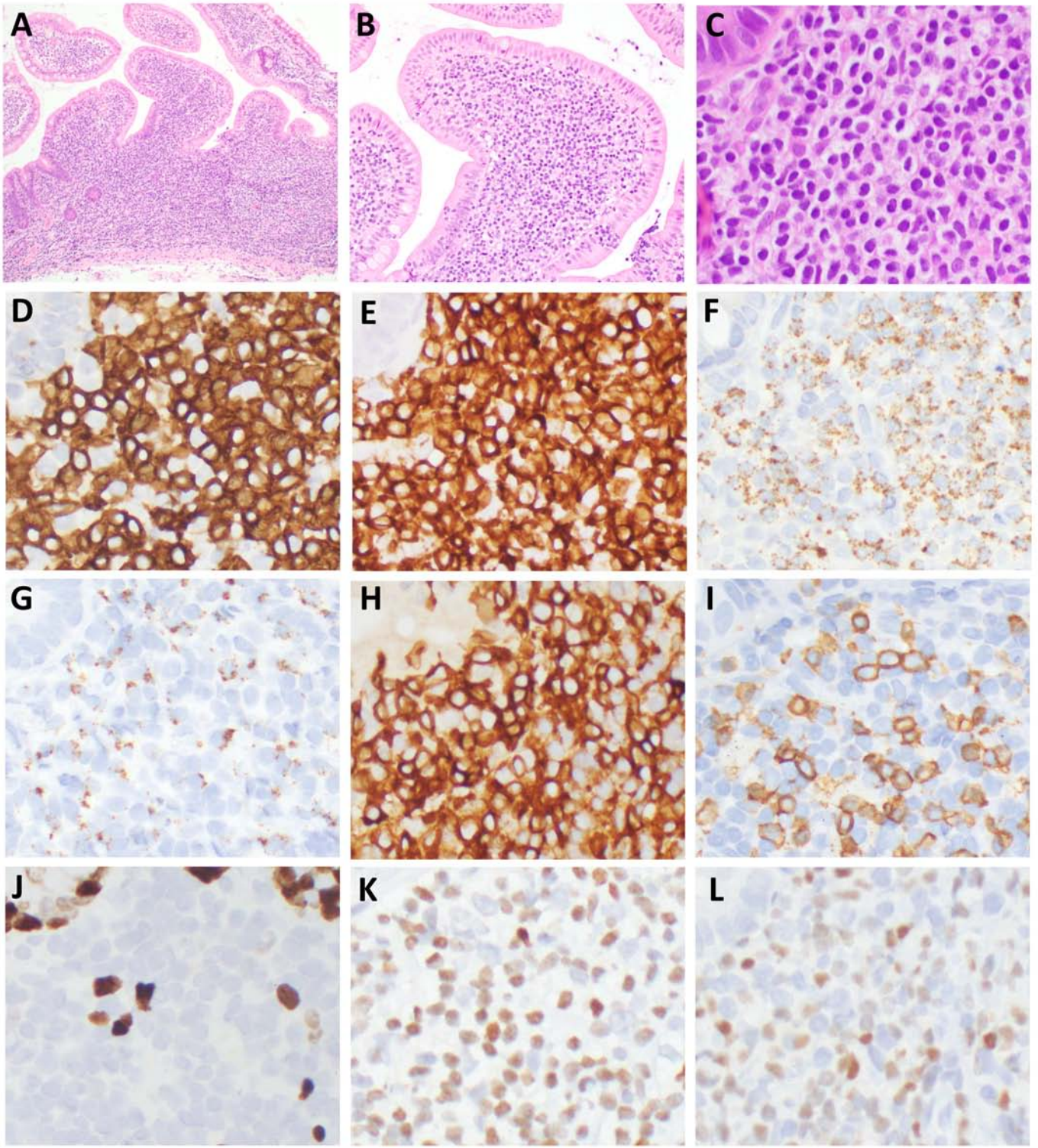
A
B
C
D
E
F
G
H
I
J
K
L

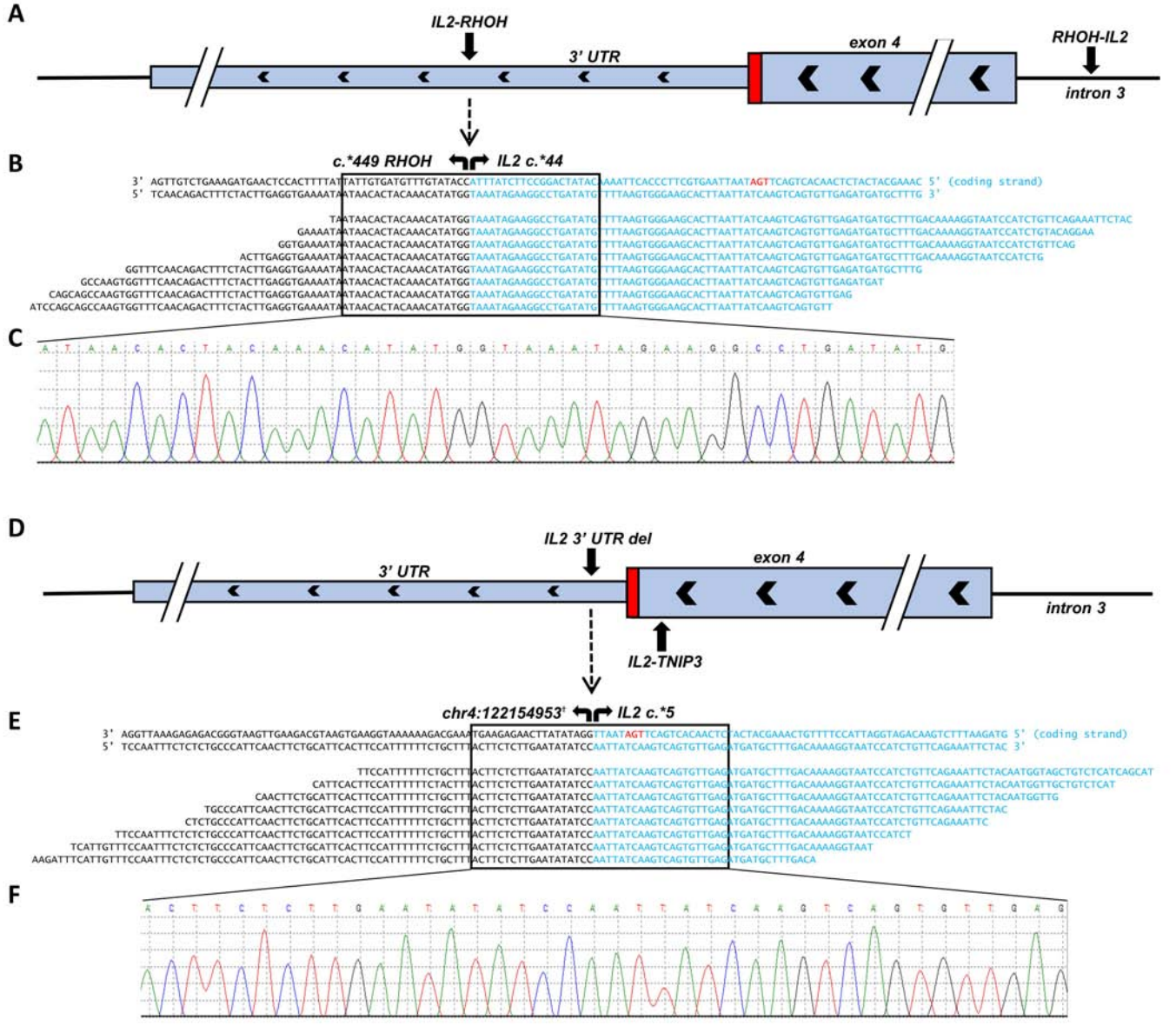
A
IL2-RHOH
3' UTR
exon 4
RHOH-IL2
intron 3
B
c.*449 RHOH
IL2 c.*44
3' AGTTGTCTGAAAGATGAACTCCACTTTTATTATTGTGATGTTTGTATACCATTTATCTTCCGGACTATACAAATTCACCCTTCGTGAATTAATAGTTCAGTCACAACTCTACTACGAAAC 5' (coding strand)
5' TCAACAGACTTTCTACTTGAGGTGAAAATAATAACACTACAAACATATGGTAAATAGAAGGCCTGATATGTTTAAGTGGGAAGCACTTAATTATCAAGTCAGTGTTGAGATGATGCTTTG 3'
TAATAACACTACAAACATATGGTAAATAGAAGGCCTGATATGTTTAAGTGGGAAGCACTTAATTATCAAGTCAGTGTTGAGATGATGCTTTGACAAAAGGTAATCCATCTGTTCAGAAATTCTAC
GAAAATAATAACACTACAAACATATGGTAAATAGAAGGCCTGATATGTTTAAGTGGGAAGCACTTAATTATCAAGTCAGTGTTGAGATGATGCTTTGACAAAAGGTAATCCATCTGTACAGGAA
GGTGAAAATAATAACACTACAAACATATGGTAAATAGAAGGCCTGATATGTTTAAGTGGGAAGCACTTAATTATCAAGTCAGTGTTGAGATGATGCTTTGACAAAAGGTAATCCATCTGTTCAG
ACTTGAGGTGAAAATAATAACACTACAAACATATGGTAAATAGAAGGCCTGATATGTTTAAGTGGGAAGCACTTAATTATCAAGTCAGTGTTGAGATGATGCTTTGACAAAAGGTAATCCATCTG
GGTTTCAACAGACTTTCTACTTGAGGTGAAAATAATAACACTACAAACATATGGTAAATAGAAGGCCTGATATGTTTAAGTGGGAAGCACTTAATTATCAAGTCAGTGTTGAGATGATGCTTTG
GCCAAGTGGTTTCAACAGACTTTCTACTTGAGGTGAAAATAATAACACTACAAACATATGGTAAATAGAAGGCCTGATATGTTTAAGTGGGAAGCACTTAATTATCAAGTCAGTGTTGAGATGAT
CAGCAGCCAAGTGGTTTCAACAGACTTTCTACTTGAGGTGAAAATAATAACACTACAAACATATGGTAAATAGAAGGCCTGATATGTTTAAGTGGGAAGCACTTAATTATCAAGTCAGTGTTGAG
ATCCAGCAGCCAAGTGGTTTCAACAGACTTTCTACTTGAGGTGAAAATAATAACACTACAAACATATGGTAAATAGAAGGCCTGATATGTTTAAGTGGGAAGCACTTAATTATCAAGTCAGTGTT
C
D
IL2 3' UTR del
3' UTR
exon 4
intron 3
IL2-TNIP3
E
chr4:122154953†
IL2 c.*5
3' AGGTTAAAGAGAGACGGGTAAGTTGAAGACGTAAGTGAAGGTAAAAAAGACGAAATGAAGAGAACTTATATAGGTTAATAGTTCAGTCACAACTCTACTACGAAACTGTTTTCCATTAGGTAGACAAGTCTTTAAGATG 5' (coding strand)
5' TCCAATTTCTCTCTGCCCATTCAACTTCTGCATTCACTTCCATTTTTTCTGCTTTACTTCTCTTGAATATATCCAATTATCAAGTCAGTGTTGAGATGATGCTTTGACAAAAGGTAATCCATCTGTTCAGAAATTCTAC 3'
TTCCATTTTTTCTGCTTTACTTCTCTTGAATATATCCAATTATCAAGTCAGTGTTGAGATGATGCTTTGACAAAAGGTAATCCATCTGTTCAGAAATTCTACAATGGTAGCTGTCTCATCAGCAT
CATTCACTTCCATTTTTTCTACTTTACTTCTCTTGAATATATCCAATTATCAAGTCAGTGTTGAGATGATGCTTTGACAAAAGGTAATCCATCTGTTCAGAAATTCTACAATGGTTGCTGTCTCAT
CAACTTCTGCATTCACTTCCATTTTTTCTGCTTTACTTCTCTTGAATATATCCAATTATCAAGTCAGTGTTGAGATGATGCTTTGACAAAAGGTAATCCATCTGTTCAGAAATTCTACAATGGTTG
TGCCCATTCAACTTCTGCATTCACTTCCATTTTTTCTGCTTTACTTCTCTTGAATATATCCAATTATCAAGTCAGTGTTGAGATGATGCTTTGACAAAAGGTAATCCATCTGTTCAGAAATTCTAC
CTCTGCCCATTCAACTTCTGCATTCACTTCCATTTTTTCTGCTTTACTTCTCTTGAATATATCCAATTATCAAGTCAGTGTTGAGATGATGCTTTGACAAAAGGTAATCCATCTGTTCAGAAATTC
TTCCAATTTCTCTCTGCCCATTCAACTTCTGCATTCACTTCCATTTTTTCTGCTTTACTTCTCTTGAATATATCCAATTATCAAGTCAGTGTTGAGATGATGCTTTGACAAAAGGTAATCCATCT
TCATTGTTTCCAATTTCTCTCTGCCCATTCAACTTCTGCATTCACTTCCATTTTTTCTGCTTTACTTCTCTTGAATATATCCAATTATCAAGTCAGTGTTGAGATGATGCTTTGACAAAAGGTAAT
AAGATTTCATTGTTTCCAATTTCTCTCTGCCCATTCAACTTCTGCATTCACTTCCATTTTTTCTGCTTTACTTCTCTTGAATATATCCAATTATCAAGTCAGTGTTGAGATGATGCTTTGACA
F

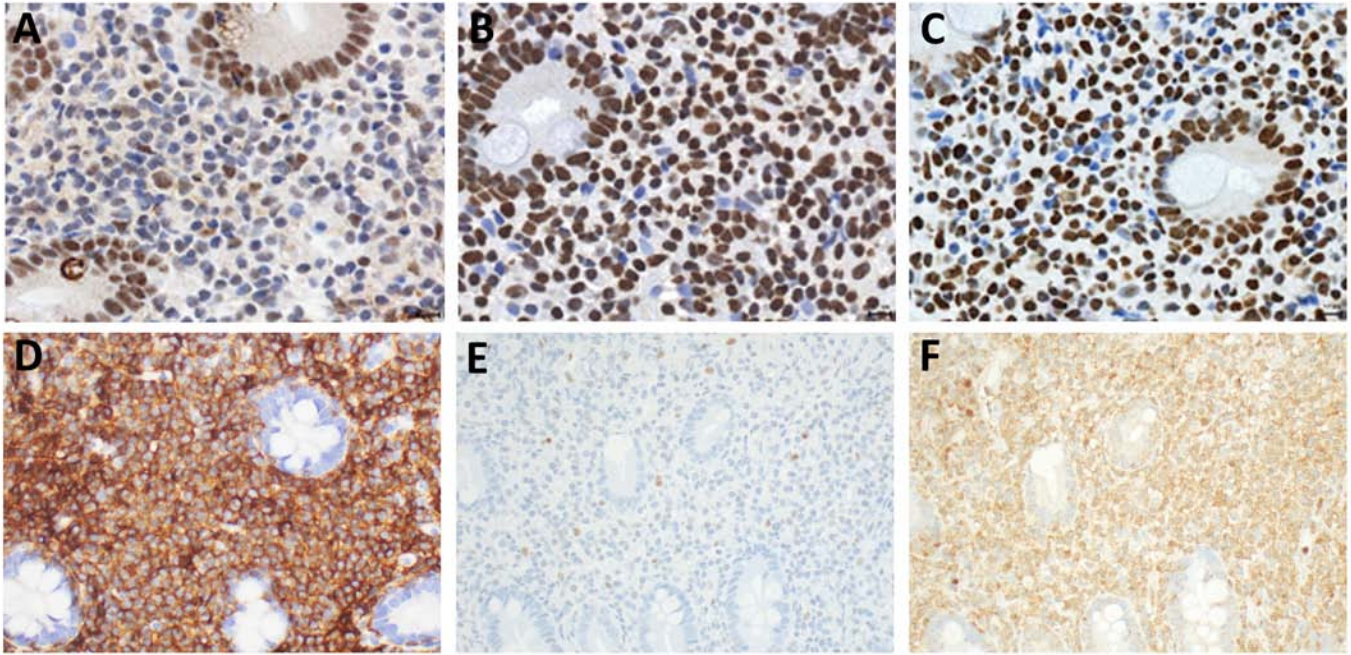
A
B
C
D
E
F

Supplementary Methods

Immunohistochemistry

Immunohistochemical (IHC) staining was performed using the following primary antibodies: CD3, CD5, CD8, CD20 and CD30 (DAKO, Carpinteria, CA); CD2, CD7, CD25 and CD56, (Vector, Burlingame, CA); CD4 (BioGenex, San Ramon, CA); TCRγ (ThermoFisher, Waltham, MA); perforin (Novocastra, Newcastle Upon Tyne, UK); granzyme-B (Chemicon, Temecula, CA); T-cell intracellular antigen-1 (TIA-1) (Beckman Coulter, Fullerton, CA); Ki-67 (Ventana, Tucson, AZ); PD1 (Cell Marque, Rocklin, CA); CD103, FoxP3, H3K36me3, H3K36me2 (Abcam, Cambridge, MA), GATA3 (Biocare Medical, Pacheco, CA), T-bet, p-STAT3(Tyr705)(clone D3A7) (Cell Signaling Technologies, Danvers, MA), p-STAT5(Tyr694/9)(clone Y694/99) (Advantex BioReagents, Houston, TX), MATK(LSK)(clone H-1) (Santa Cruz Biotechnology, Dallas, TX) and SETD2 (Sigma, Darmstadt, Germany). Staining for pSTAT5 was performed on a Benchmark Ultra autostainer (Ventana). After heat-induced epitope retrieval (Tris based pH = 9.0), slides were incubated with the antibody (1:50 dilution) for 32 minutes at 37°C; Optiview DAB kit (Ventana) was used for visualization. Staining for pSTAT3 was performed on a Discovery Ultra autostainer (Ventana). After heat-induced epitope retrieval (Tris based pH = 9.0), slides were incubated with antibody (1:25 dilution) for 2 hours at room temperature; ChromoMap DAB kit (Ventana) was used for visualization. MATK staining was performed on a Bond Max autostainer (Leica Biosystems, Bannockburn, IL, USA). After heat-induced epitope retrieval (EDTA based pH = 9.0), slides were incubated with antibody (dilution of 1:200) for 15 minutes; Bond Polymer Refine detection kit (Leica) was used for visualization. For SETD2 and H3K36, IHC was performed manually after heat-induced antigen retrieval (Tris/EDTA pH = 9.0) as previously described[17]. All other IHC staining was performed according to standard protocols on a Bond III autostainer (Leica) after online-automated heat epitope induced retrieval and the Bond Polymer Refine detection kit was used for visualization.

Flow cytometry

Four or eight color flow cytometry was performed on cell suspensions prepared from tissue samples (FACScan; Becton Dickinson, San Diego, CA) and data were analyzed using FCS Express software (De Novo Software, Los Angeles, CA) according to standard procedures. The antigens evaluated included CD45, CD2, CD3 (cytoplasmic and surface), CD4, CD5, CD7, CD8, CD30, CD56, CD20, CD25, CD43, CD103, PD1, TCRαβ and TCRγδ.

Validation of chromosomal structural alterations

PCR amplification of the DNA breakpoints and Sanger sequencing was performed on the tumor and matched normal samples. M13-tailed case-specific primers were designed to span the identified breakpoints. PCR was performed using 50 ng sample DNA, 30 ng of each specific primer, and Platinum Taq High Fidelity DNA polymerase (Invitrogen, ThermoFisher Scientific, Pittsburgh, PA). Thermal cycling conditions were one cycle at 94 C for five minutes; followed by 35 cycles at 94 C for 60s, 55 C for 90s, 68 C for 60s; followed by 68 C for 5 min. Products were used as templates for bidirectional BigDyeTerminator V1.1 Sanger sequencing (Applied Biosystems, ThermoFisher Scientific, Pittsburgh, PA).

Supplementary Tables

Supplementary Table 1: Quantification of T-bet and GATA3 expression.

Case	*Phenotype*	*T-bet (% positive)*	*GATA3 (% positive)*
1	CD4+	100%	20%
2	CD4+	100%	50%
3	CD4+	20%	100%
4	CD4+	100%	100%
5	CD4+/CD8+	50%	100%
6	CD4-/CD8-	5%	100%
7	CD8+	20%	100%
8	CD8+	60%	100%
9	CD8+	10%	100%
10	CD8+	20%	100%

Supplementary Table 2: Variants of Uncertain Significance

Case	Gene	Transcript	Chrm	Position	Total Reads	Alt Reads	Ref Base	Alt Base	AA Change	Base Change
4	FAT1	NM_005245	4	187628173	601	45	G	A	R937X	c.2809C>T
4	FOXL2	NM_023067	3	138665048	213	16	C	G	A173P	c.517G>C
4	KAT6A	NM_001099412	8	41790108	1397	109	C	T	R1877H	c.5630G>A
4	KDM5C	NM_004187	X	53223826	626	122	G	A	S1178L	c.3533C>T
4	KDM5C	NM_004187	X	53223844	587	119	G	T	P1172H	c.3515C>A
4	KMT2D	NM_003482	12	49415596	276	24	A	C	C5527W	c.16581T>G
4	RBM10	NM_001204468	X	47032564	291	53	G	A	R222Q	c.665G>A
6	MED12	NM_005120	X	70339981	684	117	G	A	E172K	c.514G>A
6	TET2	NM_001127208	4	106164741	438	130	C	G	S1203R	c.3609C>G
7	PDGFRA	NM_006206	4	55143621	491	26	C	A	S618Y	c.1853C>A
7	POLE	NM_006231	12	133256236	488	25	G	T	P142Q	c.425C>A
8	FAT1	NM_005245	4	187524362	737	42	C	T	R3773H	c.11318G>A
9	ROS1	NM_002944	6	117714432	1146	253	G	A	P406L	c.1217C>T

Supplementary Table 3: SETD2-H3K36me3 and pSTAT3/pSTAT5 Immunohistochemical Analysis

Case	*SETD2 FISH*	*SETD2 IHC*	*H3K36me2*	*H3K36me3*	*pSTAT3 (Y705)*	*pSTAT5 (Y694)*
1	-	+	+	+	-	-
2	-	+	+	+	-	-
3	NP	NP	NP	NP	-	-
4	-	+	+	+	-	-
5	NP	NP	NP	NP	-	-
6	-	+	+	+	-	NP
7	-	+	+	+	-	-
8	-	+	+	+	-	-
9	-	+	+	+	-	-
10	NP	NP	NP	NP	NP	NP
TOTAL	0/7 0%	7/7 (100%)	7/7 (100%)	7/7 (100%)	0/9 (0%)	0/8 (0%)
CD4+	0/3 (0%)	3/3 (100%)	3/3 (100%)	3/3 (100%)	0/4 (0%)	0/4 (0%)
DP	NP	NP	NP	NP	0/1 (0%)	0/1 (0%)
DN	0/1 (0%)	1/1 (100%)	1/1 (100%)	1/1 (100%)	0/1 (0%)	NP
CD8+	0/3 (0%)	3/3 (100%)	3/3 (100%)	3/3 (100%)	0/3 (0%)	0/3 (0%)

+, positive; -, negative; DN, Double-negative; DP, Double-positive; NP, Not performed

Supplementary Figures

Supplementary Figure 1: T-bet and GATA3 immunohistochemistry.

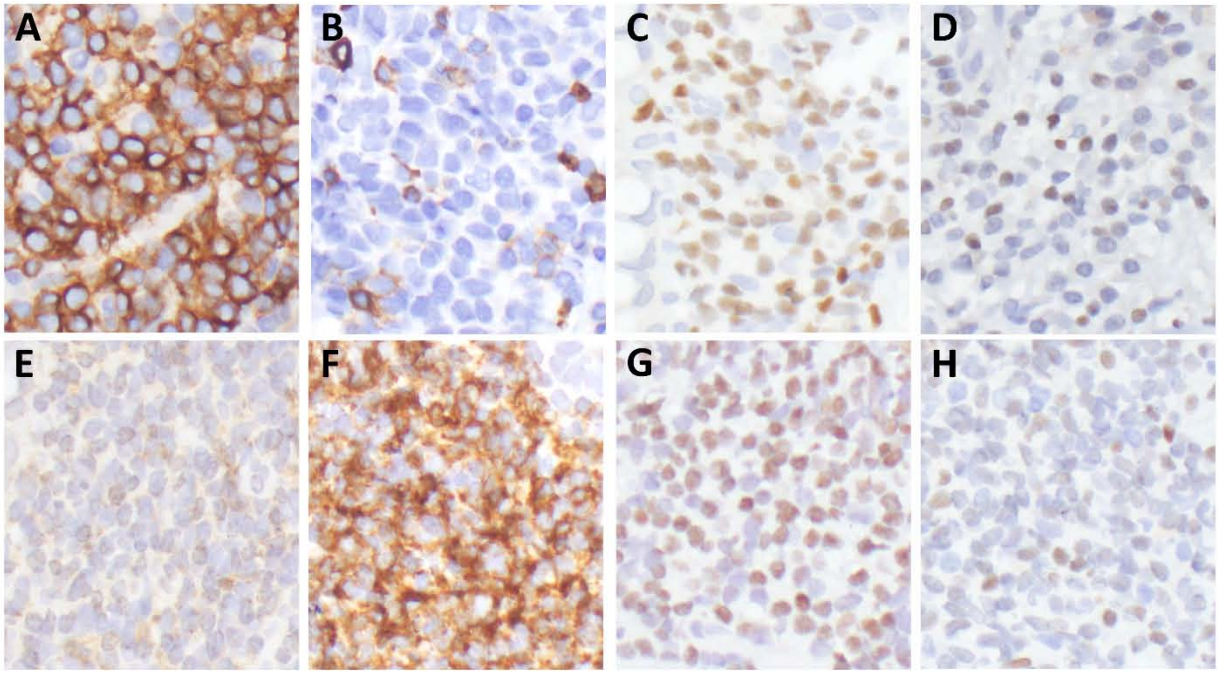

Case 1 is positive for **(A)** CD4 and negative for **(B)** CD8. **(C)** T-bet is expressed by the majority and **(D)** GATA3 is expressed by 20% of cells.

Case 9 is negative for **(E)** CD4 and positive for **(F)** CD8. **(G)** GATA3 is expressed by virtually all the cells and **(H)** T-bet is expressed by 10% of cells.